Submitted to Journal of Materials Research & Technology (February 2016)

Achieving superplastic properties in a ZK10 magnesium alloy processed by equal-channel angular pressing

Roberto B. Figueiredo[1,*], Terence G. Langdon[2,3]

[1] Department of Materials Engineering and Civil Construction, Universidade Federal de Minas Gerais, Belo Horizonte, MG 31270-901, Brazil
[2] Materials Research Group, Faculty of Engineering and the Environment, University of Southampton, Southampton SO17 1BJ, U.K.
[3] Departments of Aerospace & Mechanical Engineering and Materials Science, University of Southern California, Los Angeles, CA 90089-1453, U.S.A.

Abstract: Equal-channel angular pressing provides an opportunity for refining the grain structure and introducing superplastic properties in magnesium alloys. This report describes the use of this processing technique with a ZK10 (Mg-1.0 wt.% Zn-0.26 wt.% Zr) alloy. The grain structure was successfully refined from ~12.9 to ~5.2 μm after 4 passes and superplastic elongations were observed when testing at low strain rates at temperatures of 473 and 523 K. An analysis shows that the superplastic behavior is consistent with the conventional theoretical model for superplastic flow and at higher stresses and strain rates there is a transition to control by a viscous glide process.
Keywords: equal-channel angular pressing; magnesium alloy; superplasticity; viscous glide; ZK10.
[*]corresponding author: figueiredo@demc.ufmg.br (+55) 31 3409-1751

1. Introduction

Magnesium and its alloys usually exhibit low ductility at low temperatures and this is due to the limited number of active slip systems that are available to accommodate the plastic deformation. It is well established that an increasing temperature leads to the activation of additional slip systems thereby improving the formability of these materials [1]. Furthermore, provided the grain structure is sufficiently fine, with average grain sizes smaller than ~10 μm, a significant portion of the plastic deformation may arise from grain boundary sliding (GBS) at high temperatures [2]. The occurrence of GBS is linked to a high value of the strain rate sensitivity which inhibits strain localization and permits the material to pull out in tension to very large superplastic elongations without failure. This superplastic flow is important in industrial applications because it provides an opportunity to produce complex curved shapes through simple forming operations [3].

Superplasticity is a diffusion-controlled process requiring both a fine grain size and a high testing temperature, typically above ~0.5T_m where T_m is the absolute melting temperature. At these high temperatures, a fine grain size is most easily retained through the presence of second phase precipitates and in magnesium alloys superplasticity has been reported in alloys containing precipitates such as AZ61 [4,5] and ZK60 [6]. Also, the material must be processed in order to obtain a fine-grained structure and this is generally undertaken using powder metallurgy techniques [7]. More recently, the development of processing procedures based on the application of severe plastic deformation (SPD) has provided opportunities for achieving exceptional grain refinement in many metallic alloys, including magnesium alloys, together with significant superplastic properties [8].

Although there are several different SPD processing methods, most attention to date has focused on equal-channel angular pressing (ECAP) where a rod or bar is pressed through a die constrained within a channel [9] or high-pressure torsion (HPT) where a thin disk is subjected to compression and concurrent torsional straining [10]. Comprehensive reviews are now available documenting the experimental data reported for superplasticity in alloys processed using ECAP and HPT [11-13]. Initially, significant attention was given to the ZK60 alloy (Mg- 5.5 wt.% Zn-0.5 wt.% Zr) which exhibits excellent superplastic properties after processing by ECAP [14-21] including a potential for attaining high strain rate superplasticity [21] and the development of a record superplastic elongation of more than 3000% [19]. In addition to the excellent superplastic properties recorded in the ZK60 alloy, other magnesium alloys also exhibit superplasticity after processing by ECAP including the single phase AZ31 alloy [22-26]. However, despite the excellent superplastic properties introduced in a single phase magnesium alloy having aluminum in solid solution, there has been only limited research to date to evaluate the potential for achieving superplasticity in other dilute magnesium alloys. For example, it was reported recently that ECAP processing leads to low temperature superplasticity in a ZM21 (Mg-1.78 wt.% Zn-0.89 wt.% Mn) alloy [27].

Accordingly, the present research was initiated to evaluate the potential for achieving superplastic ductilities in a more dilute ZK10 alloy (Mg-1.0 wt.% Zn-0.25 wt.% Zr). This alloy was selected because excellent superplastic properties were already reported in the ZK60 magnesium alloy which has a much higher zinc content and both ZK60 and ZK10 have zinc and zirconium as the major alloying elements. As will be demonstrated, superplastic properties are also attained in the ZK10 alloy but the elongations are significantly lower than in the ZK60 alloy.

2. Experimental material and procedures

The experiments were conducted using a magnesium ZK10 alloy supplied by Magnesium Elektron (Riverside, CA) as rolled slabs. The composition of the alloy is shown in Table 1. Billets with diameters of 10 mm and lengths of 60 mm were machined from the slabs with the axial directions parallel to the rolling direction. These billets were processed by ECAP at a temperature of 493 K using a die with an angle of 110° between the two channels and with an outer arc of curvature of 20° at the intersection of the two channels. These angles in the ECAP die produce a strain of ~0.8 on each separate pass through the die [28] and the billets were processed for up to 4 passes using route B_c in which the billet is rotated by 90° in the same sense between each pass [29].

Samples of the material were extracted before and after ECAP processing for metallography. The samples were ground on silica carbide papers and polished to a mirror-like finish on cloth using alumina oxide and ethanol as abrasive media. The grain boundaries were revealed by etching with acetic-picral (70 mL of ethanol, 4.2 g of picric acid, 10 mL of acetic acid and 10 mL of water). The average grain size was determined as $d = 1.74 \times L$ where L is the mean intercept length.

Tensile specimens with gauge lengths of 4 mm and cross-sections of 2×3 mm^2 were machined from the processed billets and tested in tension at different temperatures and strain rates. Load and displacement data were converted to true stress-true strain curves by assuming volume constancy and homogeneous deformation. The machine elastic distortion was corrected by equating the elastic region of the curve to the theoretical elastic modulus of the material.

3. Experimental results

3.1 Grain structure after ECAP

Figure 1 shows representative images of the grain structures of the material before and after processing by ECAP. It was observed that etching does not reveal all of the grain boundaries with the same intensity. Thus, some boundaries are readily visible and others are poorly defined. The average grain size in the as received condition in Fig. 1(a) was measured as ~12.9 μm. Processing by ECAP promoted significant grain refinement. After only 2 passes in Fig. 2(b) the structure became bimodal with some larger grains and areas of smaller grains of a few micrometers. This bimodal grain size distribution is generally expected in magnesium alloys due to the mechanism of grain refinement in which new fine grains are formed preferentially along the grain boundaries while the cores of the original grains remain unrefined [30,31]. After 2 passes the average grain size was ~6.8 μm. Similar features were also observed in the alloy after 4 passes of ECAP as shown in Fig. 1(c) where the average grain size was slightly smaller at $d \approx 5.2$ μm.

3.2 Tensile testing

Tensile tests were carried out at different temperatures in the range from 473 to 573 K after processing through 4 passes of ECAP. Figure 2 shows the recorded elongations when testing with an initial strain rate of 1.0×10^{-4} s^{-1} plotted as a function of the testing temperature, T. Thus, high elongations of ~500% are observed at 473 and 493 K and there is a peak elongation of 750% at 523 K. Thereafter, there is a sharp reduction in elongation to <400% at 573 K due to the advent of grain growth at this higher temperature. Superplasticity is defined formally as elongations in tension of at least 400% [32] and therefore these results show

there is a capability for achieving superplastic flow in the ZK10 alloy at temperatures up to ~540 K.

Tensile tests were also carried out on samples of the material processed by only 2 passes of ECAP and Fig. 3(a) shows plots of true stress and true strain for tests conducted at temperatures of 473 and 523 K for tests at an initial strain rate of 1.0×10^{-3} s^{-1}. Also shown in Fig. 3(a) are curves for samples tested under these conditions after 4 passes of ECAP. Inspection shows processing through 4 passes leads to lower flow stresses at both temperatures. This difference in flow stress is due to the finer grain size achieved in the material after processing through 4 passes.

Similar stress-strain curves are shown in Fig. 3(b) for tests conducted on the material processed for 4 passes of ECAP at different initial strain rates from 10^{-4} to 10^{-2} s^{-1} and at the two temperatures of 473 and 523 K. It is readily observed that the flow stress varies significantly with the imposed strain rate thereby indicated a high strain rate sensitivity. The curves obtained at 523 K also exhibit lower flow stresses compared to their counterparts at 473 K. Nevertheless, it is important to note that all curves exhibit a significant increase in flow stress with increasing strain. Similar behavior was also reported in earlier experiments on a ZK60 magnesium alloy and it was attributed to the occurrence of grain growth [33].

The appearance of typical specimens after failure are shown in Fig. 4, together with the recorded final elongations, where all samples were processed by ECAP through 4 passes and the tests were conducted at 473 K in Fig. 4(a) and at 523 K in Fig. 4(b): for both illustrations, an untested initial sample is shown at the top. Elongations of >400% in the superplastic range are observed at the lower initial strain rates of 10^{-4} to 10^{-3} s^{-1} at both testing temperatures and it is noted that the elongation of 390% observed at a high strain rate of 10^{-2} s^{-1} at 523 K is only slightly outside of the conventional range for superplasticity. In the superplastic regime, as at an initial strain rate of 1.0×10^{-4} s^{-1} at 523 K, the specimens exhibit a constant thinning of the cross-sectional area and gradually pull out to failure at a point as expected for true superplastic deformation where the high strain rate sensitivity prevents strain localization and the development of sharp necking within the gauge length [34]. By contrast, very clear necking was observed at the highest strain rate of 1.0×10^{-2} s^{-1} at 473 K where the total elongation was only 180%.

4. Discussion

These results confirm that processing by ECAP is effective in significantly refining the grain structure of the ZK10 magnesium alloy. The initial coarser structure of ~12.9 μm was successfully refined to an average spatial grain size of ~5.2 μm after 4 passes. Although this is larger than the average grain size observed in other metallic materials after processing by ECAP, it is within the range of grain sizes observed in magnesium alloys in which processing takes place at higher temperatures. Also, the grain size is usually reported as the mean linear intercept length and this is smaller than the spatial average grain size. It was shown earlier that the mean linear intercept grain size was ~2.2 μm in an AZ31 magnesium alloy processed by 4 passes of ECAP at 473 K using a die with 110^{o} between channels and this is equivalent to a spatial grain size of ~3.8 μm [24].

There are some reports of finer grain sizes in magnesium alloys processed by ECAP, including the development of true ultrafine-grained structures but in practice the final grain size is strongly affected by the initial grain structure prior to the ECAP processing [31]. It is also well established that grain sizes smaller than 1 μm may be

attained by processing the magnesium alloys using HPT: for example, in HPT processing there are reports of average grain sizes of 230 nm in AZ31 [35], 210 nm in Mg-9Al [36], 85 nm in Mg-9Gd-4Y-0.4Zr [37], 100 nm in Mg-10Gd [38], 500 nm in Mg-8Li [39] and 700 nm [40] and 900 nm [41,42] in ZK60.

The level of grain refinement achieved in the present experiments is within the range in which superplasticity is expected (d < 10 μm) [43] and the occurrence of superplastic flow was confirmed by tensile testing at different temperatures and strain rates where excellent elongations were observed up to a maximum of 750%. It is important, therefore, to analyze the characteristics of the flow process.

At high temperatures, the flow process of metals is described by a relationship of the form [43]:

$$\dot{\varepsilon} = \frac{AGb}{kT} D_0 \exp\left(\frac{-Q}{RT}\right)\left(\frac{b}{d}\right)^p \left(\frac{\sigma}{G}\right)^n \qquad (1)$$

where $\dot{\varepsilon}$ is the effective strain rate, A is a dimensionless constant, G is the shear modulus, b is the Burgers vector modulus, k is the Boltzmann's constant, T is the absolute temperature, D_0 is a frequency factor, Q is the activation energy for the flow process, R is the gas constant, σ is the applied stress, p is the inverse grain size exponent and n is the stress exponent. In conventional metals, the rate-controlling mechanism for superplasticity is grain boundary sliding [44] which is accommodated by limited amounts of intragranular slip [45]. A theoretical model for the superplastic sliding process leads to eq. (1) with A = 10, p = 2, n = 2, and an activation energy equal to the value for grain boundary diffusion [46]. For magnesium, this gives $Q \approx$ 92 kJ mol^{-1} [47].

The stress exponent is the inverse of the strain rate sensitivity and this may be determined by logarithmically plotting the strain rate, for a selected fixed temperature and grain size, as a function of stress. An example is shown in Fig. 5(a) and the slope of the line is the stress exponent so that $n \approx 3.3$ for specimens processed through 4 passes of ECAP and tested at 473 and 523 K.

The activation energy for the flow process may be determined using the relationship [48]

$$Q = nR\left[\frac{\partial \ln \sigma}{\partial\left(\frac{1}{T}\right)}\right]_{d,\dot{\varepsilon}(\text{const})} \qquad (2)$$

Thus, considering the same grain size for tests at temperatures of 473 and 523 K, the activation energy is obtained by plotting the flow stresses observed at similar strain rates, using a logarithmic scale, as a function of the inverse of the testing temperature. This plot is shown in Fig. 5(b) where the slope is equal to Q/nR so that, taking the experimental value of n = 3.3, the measured activation energy is Q ≈ 112 kJ mol^{-1}. This value lies between the expected activation energies for lattice diffusion (~135 kJ mol^{-1}) and grain boundary diffusion (~92 kJ mol^{-1}) [47].

This analysis shows that, although the grain size is within the anticipated range for superplastic flow and the experimental elongations are >400% and within the regime of superplasticity, the stress exponent of n ≈ 3.3 is not consistent with the theoretical model for superplasticity where n = 2. Nevertheless, the reduction in flow stress observed in the stress-strain curves for samples processed by 4 passes compared to samples processed by only 2 passes suggests that grain size plays a

role in the deformation mechanism which also supports the experimental evidence for the occurrence of grain boundary sliding.

Therefore, in order to further check the present experimental data against the theoretical prediction for grain boundary sliding in superplasticity, the strain rate was normalized by temperature and grain size using the activation energy for grain boundary diffusion and $p = 2$ and then plotted against the normalized stress, σ/G. For this analysis, the grain boundary diffusion coefficient was taken as δD_{gb} where δ is the grain boundary width equal to $2b$ where $b = 3.21 \times 10^{-10}$ m, $\delta D_{gb} = 5.0 \times 10^{-12}$ exp (-92,000/RT) $m^3 s^{-1}$ [47] and $G = (1.92 \times 10^4 - 8.6T)$ MPa where T is the relevant temperature in degrees Kelvin [49]. Following the theoretical model for superplasticity, the dimensionless constant A was placed equal to 10 [46]. The result is given in Fig. 6 where the solid line shows the theoretical prediction based on the model for conventional superplasticity where $n = 2$ [46] and experimental points are shown for ZK10 in this investigation and for earlier results for a ZK60 alloy which exhibited excellent superplasticity after processing by ECAP [50]. It is apparent that the data for the ZK60 alloy agree well with the theoretical prediction except at the very highest stresses and this provides support for the use of the theoretical equation for superplasticity by grain boundary sliding in magnesium alloys. It is also observed that some points of the present experiments are in excellent agreement with the theoretical prediction. Specifically, for both alloys there is very good agreement between experiment and theory at the lower stresses and strain rates where the experiments give large elongations but for the ZK10 alloy there is a clear deviation at higher stresses and faster strain rates where, as shown in Fig. 4, the behavior deviates from conventional superplasticity. Thus, the results for the ZK10 alloy suggest a transition to a different flow mechanism at the faster strain rates with a stress exponent of $n \approx 3.3$ and an activation energy of ~112 kJ mol^{-1} which is intermediate between grain boundary and lattice diffusion. This value of the stress exponent suggests a transition to control by the viscous glide of dislocations [51] and this is supported by the reasonably high elongations to failure which are a standard feature of solid solution alloys undergoing creep within the viscous glide regime [52].

It is concluded that the results in this research lie in a transition region between superplasticity and viscous glide and at the lowest stresses and strain rates the data show excellent agreement with the conventional model for superplastic flow.

5. Summary and conclusions

1. A magnesium ZK10 alloy was processed by ECAP at 493 K and then tested in tension at different temperatures and strain rates. The results show the potential for achieving good superplastic elongations at the slowest strain rates at testing temperatures of 473 and 523 K. An optimum elongation of 750% was attained at 523 K using an initial strain rate of 1.0×10^{-4} s^{-1}.
2. Plots of true stress versus true strain curves exhibit significant hardening and a high strain rate sensitivity which is consistent with the large elongations.
3. An analysis of the experimental data gave a stress exponent of $n \approx 3.3$ and activation energy which was intermediate between the values for grain boundary and lattice diffusion. There is good agreement with the theoretical prediction for superplastic flow at the lowest strain rates but at higher strain rates there is a transition to a viscous glide process.

Acknowledgements

One of the authors (RBF) was supported by CNPq – Brazil, FAPEMIG and PPGEM. This research was supported in part by the National Science Foundation of the United States under Grant No. DMR-1160966 and in part by the European Research Council under ERC Grant Agreement No. 267464-SPDMETALS.

References

[1] Máthis K, Nyilas K, Axt A, Dragomir-Cernatuscu I, Ungár T, Lukác P. The evolution of non-basal dislocations as a function of deformation temperature in pure magnesium determined by X-ray diffraction. Acta Materialia. 2004;52;2889-2894.

[2] Kawasaki M, Figueiredo RB, Langdon TG. The requirements for superplasticity with an emphasis on magnesium alloys. Advanced Engineering Materials. 2016;18;127-131.

[3] Barnes AJ. Superplastic forming 40 years and still growing. Journal of Materials Engineering Performance. 2007;16;440–454.

[4] Tsutsui H, Watanabe H, Mukai T, Kohzu M, Tanabe S, Higashi K, Superplastic deformation behavior in commercial magnesium alloy AZ61. Materials Transactions 1999;40;931-934.

[5] Chung SW, Higashi K, Kim WJ, Superplastic gas pressure forming of fine-grained AZ61 magnesium alloy sheet. Materials Science and Engineering A 2004;372;15-20.

[6] Watanabe H, Mukai T, Higashi K. Superplasticity in a ZK60 magnesium alloy at low temperatures. Scripta Materialia. 1999;40;477-484.

[7] Mabuchi M, Asahina T, Iwasaki H, Higashi K. Experimental investigation of superplastic behaviour in magnesium alloys. Materials Science and Technology. 1997;13;825-831.

[8] Figueiredo RB, Langdon TG. Fabricating Ultrafine-Grained Materials through the application of Severe Plastic Deformation: a Review of Developments in Brazil. Journal of Materials Research and Technology. 2012;1;55-62

[9] Valiev RZ, Langdon TG. Principles of equal-channel angular pressing as a processing tool for grain refinement. Progress in Materials Science 2006;51;881-981.

[10] Zhilyaev AP, Langdon TG. Using high-pressure torsion for metal processing: Fundamentals and applications. Progress in Materials Science 2008;53;893-979.

[11] Kawasaki M, Langdon TG. Principles of superplasticity in ultrafine-grained materials. Journal of Materials Science. 2007;42;1782-1796.

[12] Kawasaki M, Langdon TG. Review: Achieving superplasticity in metals processed by high-pressure torsion. Journal of Materials Science 2014;49;6487-6496.

[13] Kawasaki M, Langdon TG. Review: Achieving superplastic properties in ultrafine-grained materials at high temperatures. Journal of Materials Science 2016;51;19-32.

[14] Watanabe H, Mukai T, Ishikawa K, Higashi K. Low temperature superplasticity of a fine-grained ZK60 magnesium alloy processed by equal-channel-angular extrusion. Scripta Materialia. 2002;46;851-856.

[15] Chuvil'deev VN, Nieh TG, Gryaznov MY, Sysoev AN, Kopylov VI, Low-temperature superplasticity and internal friction in microcrystalline Mg alloys processed by ECAP. Scripta Materialia. 2004;50;861-865.

[16] Chuvil'deev VN, Nieh TG, Gryaznov MYu, Kopylov VI, Sysoev AN. Superplasticity and internal friction in microcrystalline AZ91 and ZK60 magnesium alloys processed by equal-channel angular pressing. Journal of Alloys and Compounds. 2004;378;253-257.

[17] Lapovok R, Thomson PF, Cottam R, Estrin Y. Processing routes leading to superplastic behaviour of magnesium alloy ZK60. Materials Science and Engineering A 2005;410-411;390-393.
[18] Figueiredo RB, Langdon TG. The development of superplastic ductilities and microstructural homogeneity in a magnesium ZK60 alloy processed by ECAP. Materials Science and Engineering A 2006;430;151-156.
[19] Figueiredo RB, Langdon TG. Record superplastic ductility in a magnesium alloy processed by equal-channel angular pressing, Advanced Engineering Materials. 2008;10;37-40.
[20] Figueiredo RB, Langdon TG. Factors influencing superplastic behavior in a magnesium ZK60 alloy processed by equal-channel angular pressing. Materials Science and Engineering A 2009;503;141-144.
[21] Figueiredo RB, Langdon TG. Strategies for achieving high strain rate superplasticity in magnesium alloys processed by equal-channel angular pressing. Scripta Materialia. 2009;61;84-87.
[22] Lin HK, Huang JC, Langdon TG. Relationship between texture and low temperature superplasticity in an extruded AZ31 Mg alloy processed by ECAP. Materials Science and Engineering A. 2005;402;250-257.
[23] Lapovok R, Estrin Y, Popov MV, Langdon TG. Enhanced superplasticity in a magnesium alloy processed by equal-channel angular pressing with a back-pressure. Advanced Engineering Materials. 2008;10;429-433.
[24] Figueiredo RB, Langdon TG. Developing superplasticity in a magnesium AZ31 alloy by ECAP. Journal of Materials Science 2008;43;7366-7371.
[25] Lapovok R, Estrin Y, Popov MV, Rundell S, Williams T. Enhanced superplasticity of magnesium alloy AZ31 obtained through equal-channel angular pressing with back-pressure. Journal of Materials Science 2008;43;7372-7378.
[26] Figueiredo RB, Terzi S, Langdon TG. Using X-ray microtomography to evaluate cavity formation in a superplastic magnesium alloy processed by equal-channel angular pressing. Acta Materialia. 2010;58;5737-5748.
[27] Mostaed E, Fabrizi A, Dellasega D, Bonollo F, Vedani M. Microstructure, mechanical behavior and low temperature superplasticity of ECAP processed ZM21 Mg alloy. Journal of Alloys and Compounds 2015;638;267-276.
[28] Iwahashi Y, Wang J, Horita Z, Nemoto M, Langdon TG. Principle of equal-channel angular pressing for the processing of ultrafine-grained materials. Scripta Materialia. 1996;35;143-146.
[29] Furukawa M, Iwahashi Y, Horita Z, Nemoto M, Langdon TG. The shearing characteristics associated with equal-channel angular pressing. Materials Science and Engineering A 1998;257;328-332.
[30] Figueiredo RB, Langdon TG. Principles of grain refinement in magnesium alloys processed by equal-channel angular pressing. Journal of Materials Science 2009;44;4758-4762.
[31] Figueiredo RB, Langdon TG. Grain refinement and mechanical behavior of a magnesium alloy processed by ECAP. Journal of Materials Science 2010;45;4827-4836.
[32] Langdon TG. Seventy-five years of superplasticity: historic developments and new opportunities. Journal of Materials Science 2009;44;5998-6010.
[33] Figueiredo RB, Langdon TG. Influence of the number of passes in ECAP on superplastic behavior in a magnesium alloy. Materials Science Forum 2008;584-586;170-175.

[34] Langdon TG. Fracture processes in superplastic flow. Metal Science 1982;16;175-183.
[35] Harai Y, Kai M, Kaneko K, Horita Z, Langdon TG. Microstructural and mechanical characteristics of AZ61 magnesium alloy processed by high-pressure torsion. Materials Transactions. 2008;49;76-83.
[36] Kai M, Horita Z, Langdon TG. Developing grain refinement and superplasticity in a magnesium alloy processed by high-pressure torsion. Materials Science and Engineering A 2008;488;117-124.
[37] Alizadeh R, Mahmudi R, Ngan AHW, Huang Y, Langdon TG. Superplasticity of a nano-grained Mg-Gd-Y-Zr alloy processed by high-pressure torsion. Materials Science and Engineering A 2016;651;786-794.
[38] Kulyasova OB, Islamgaliev RK, Kil'mametov AR, Valiev RZ. Superplastic behavior of magnesium-based Mg-10 wt % Gd alloy after severe plastic deformation by torsion, The Physics of Metals and Metallography. 2006;101;585-590.
[39] Matsunoshita H, Edalati K, Furui M, Horita Z. Ultrafine-grained magnesium-lithium alloy processed by high-pressure torsion: Low-temperature superplasticity and potential for hydroforming. Materials Science and Engineering A 2015;640;443-448.
[40] Torbati-Sarraf SA, Sabbaghianrad S, Langdon TG. Microstructural properties, thermal stability and superplasticity of a ZK60 alloy processed by high-pressure torsion. Letters in Materials 2015;5;287-293.
[41] Torbati-Sarraf SA, Langdon TG. Properties of a ZK60 magnesium alloy processed by high-pressure torsion. Journal of Alloys and Compounds 2014;613;357–363.
[42] Torbati-Sarraf SA, Langdon TG. Mechanical properties of ZK60 magnesium alloy processed by high-pressure torsion. Advanced Materials Research. 2014;922;767-772.
[43] Langdon TG. The mechanical properties of superplastic materials. Metallurgical Transactions. 1982;13A;689-701.
[44] Langdon TG. An evaluation of the strain contributed by grain boundary sliding in superplasticity. Materials Science and Engineering A 1994;174;225-230.
[45] Valiev RZ, Langdon TG. An investigation of the role of intragranular dislocation strain in the superplastic Pb-62% Sn eutectic alloy. Acta Metallurgica Materialia. 1993;41;949-954.
[46] Langdon TG. A unified approach to grain boundary sliding in creep and superplasticity. Acta Metallurgica Materialia. 1994;42;2437-2443.
[47] Frost HJ, Ashby MF. Deformation-Mechanism Maps: The Plasticity and Creep of Metals and Ceramics, Pergamon, Oxford, UK (1982).
[48] Mohamed FA, Langdon TG. The determination of the activation energy for superplastic flow. Physica Status Solidi (a). 1976;33;375-381.
[49] Vagarali SS, Langdon TG. Deformation mechanisms in h.c.p. metals at elevated temperatures – I. Creep behavior of magnesium. Acta Metallurgica. 1981;29;1969-1982.
[50] Figueiredo RB, Langdon TG. The characteristics of superplastic flow in a magnesium alloy processed by ECAP. International Journal of Materials Research. 2009;100;843-846.
[51] Vagarali SS, Langdon TG. Deformation mechanisms in h.c.p. metals at elevated temperatures – II. Creep behavior of a Mg-0,.8% Al solid solution alloy. Acta Metallurgica. 1982;30;1157-1170.

[52] Mohamed FA. Creep ductility in large-grained solid solution alloys. Scripta Metallurgica. 1978;12;99-102.

Figure captions:

Figure 1 – Grain structure along the cross-sections of the billets of the ZK10 alloy (a) in the as-received condition and after processing by (b) 2 and (c) 4 passes of ECAP.

Figure 2 – Elongation-to-failure plotted as a function of the testing temperature for the material processed by 4 passes of ECAP and tested at an initial strain rate of 10^{-4} s^{-1}.

Figure 3 – True stress vs true strain curves observed at 473 and 523 K (a) for the material processed by different numbers of passes of ECAP and (b) for the material processed by 4 passes and tested at different strain rates.

Figure 4 – Appearance of tensile specimens of ZK10 alloy processed by 4 passes of ECAP and pulled to failure at (a) 473 K and at (b) 523 K at different strain rates.

Figure 5 – (a) Strain rate plotted as a function of stress and (b) stress plotted as a function of the inverse of temperature.

Figure 6 – Strain rate normalized by the effect of temperature and grain size and plotted as a function of the stress normalized by the shear modulus: the theoretical prediction for grain boundary sliding in superplasticity [46] and data from an earlier report [50] are shown for comparison.

Tables:

Table 1 – Chemical element concentration (in wt.%)

Alloy	Mg	Al	Zn	Mn	Zr	Ca	Cu	Si	Ni	Fe
ZK10	Bal.	0.014	1.0	0.06	0.26	0.003	0.001	0.002	0.000	0.002

Figures:

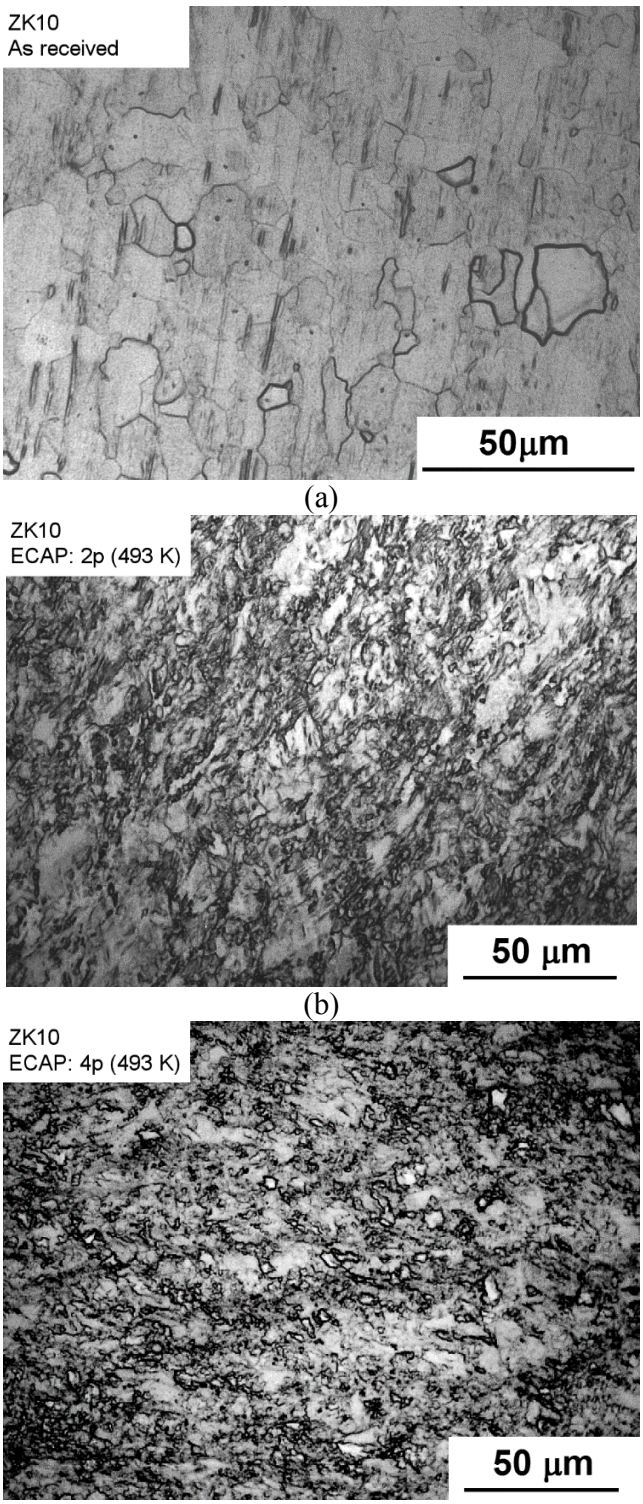

Figure 1 – Grain structure along the cross section of the billets of ZK10 alloy (a) in the as-received condition and after processing by (b) 2 and (c) 4 passes of ECAP.

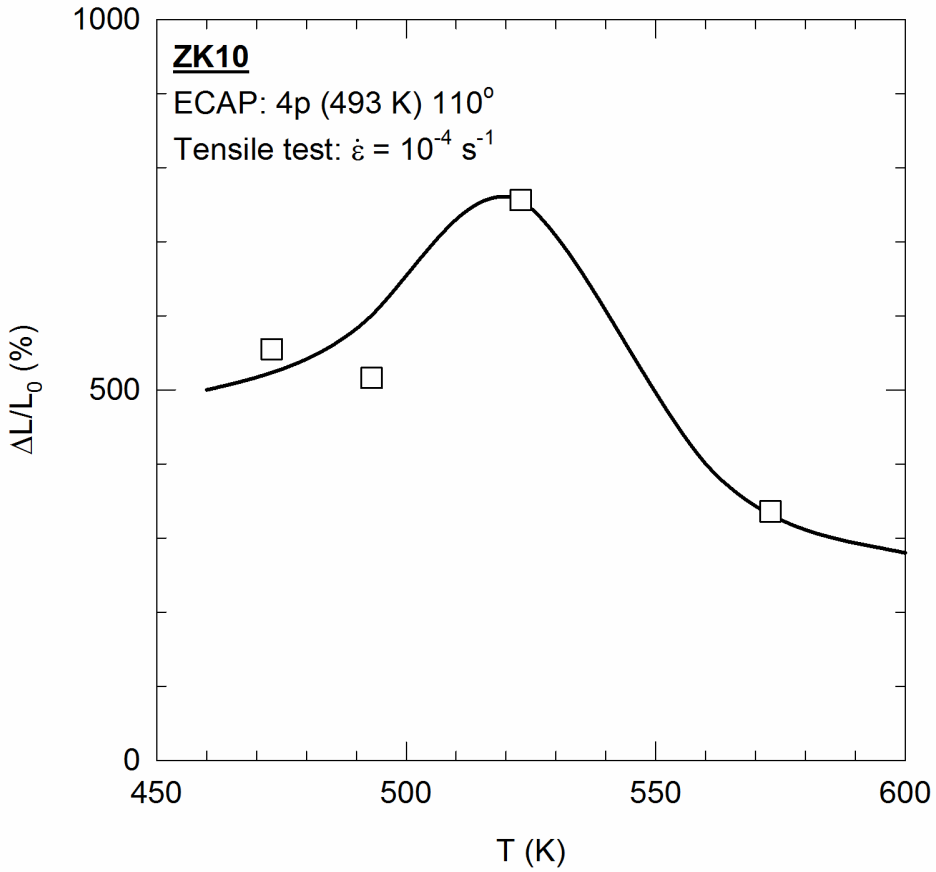

Figure 2 – Elongation-to-failure plotted as a function of the testing temperature for the material processed by 4 passes of ECAP and tested at initial strain rate of 10^{-4} s^{-1}.

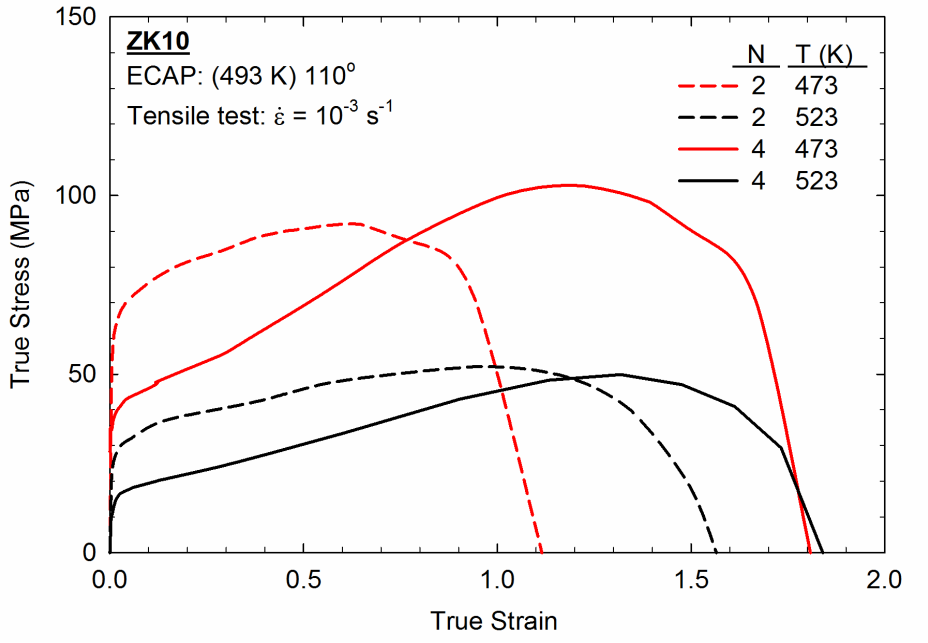

(a)

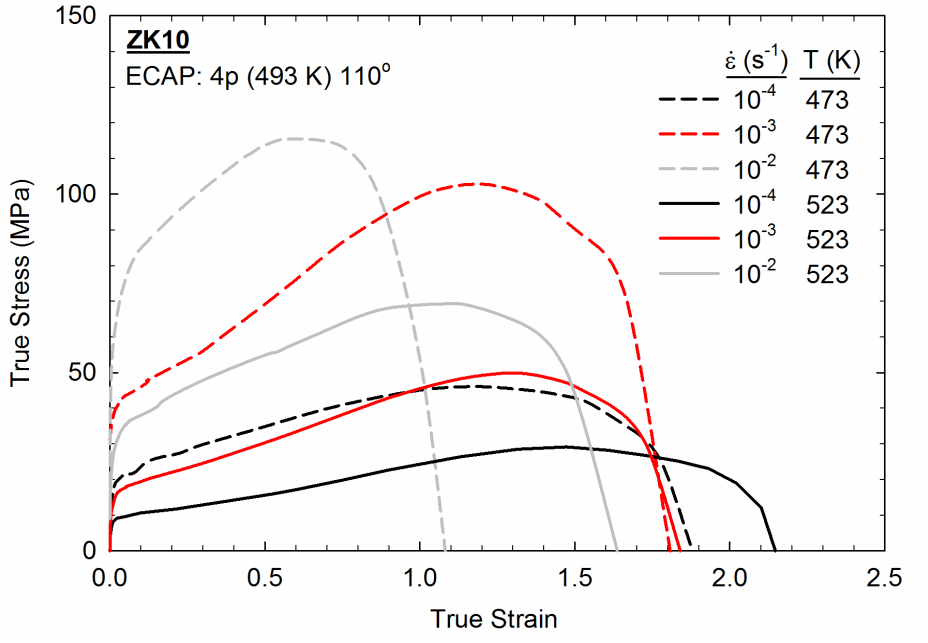

(b)

Figure 3 – True stress vs true strain curves observed at 473 K and 523 K (a) for the material processed by different number of passes of ECAP and (b) for the material processed by 4 passes and tested at different strain rates.

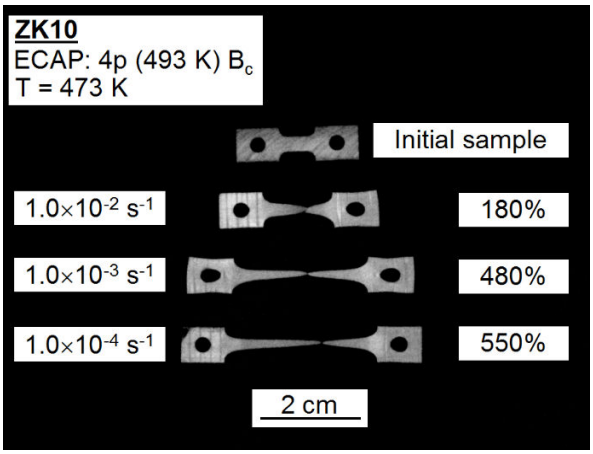

(a)

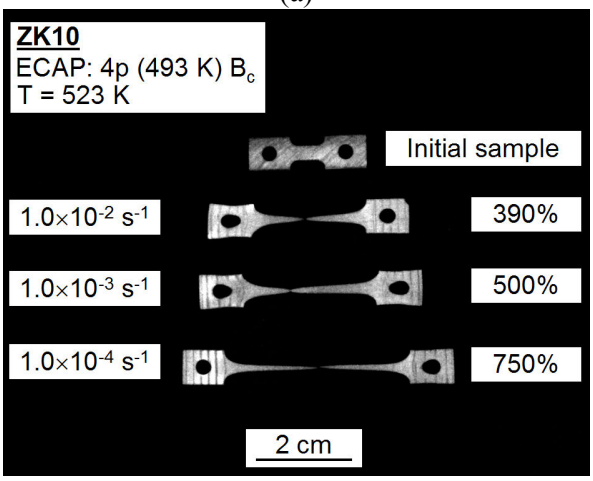

(b)

Figure 4 – Appearance of tensile specimens of ZK10 alloy processed by 4 passes of ECAP and pulled to failure at (a) 473 K and at (b) 523 K at different strain rates.

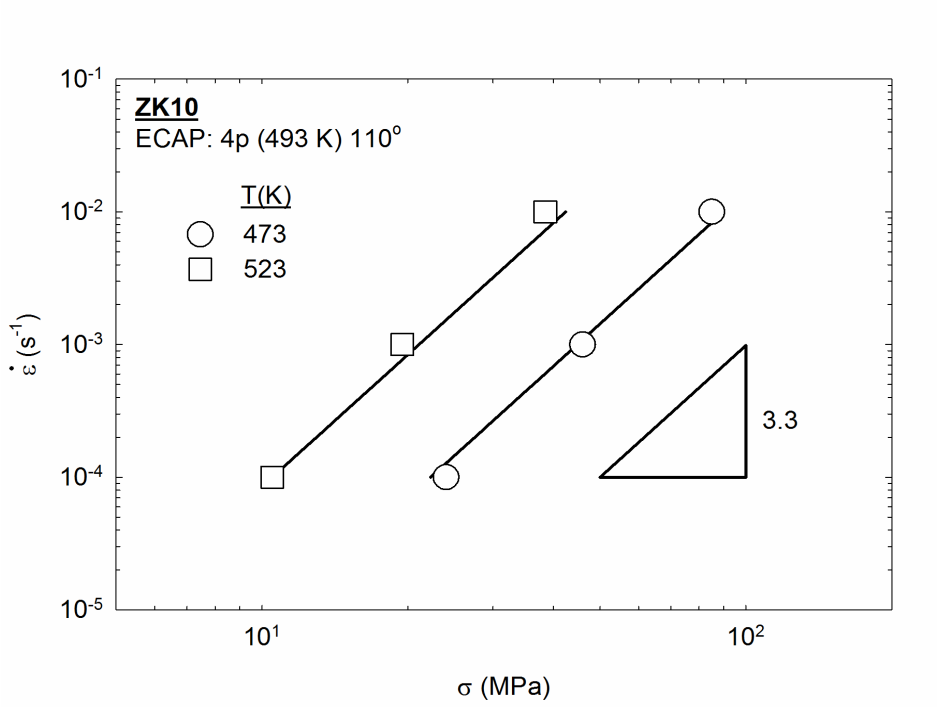

(a)

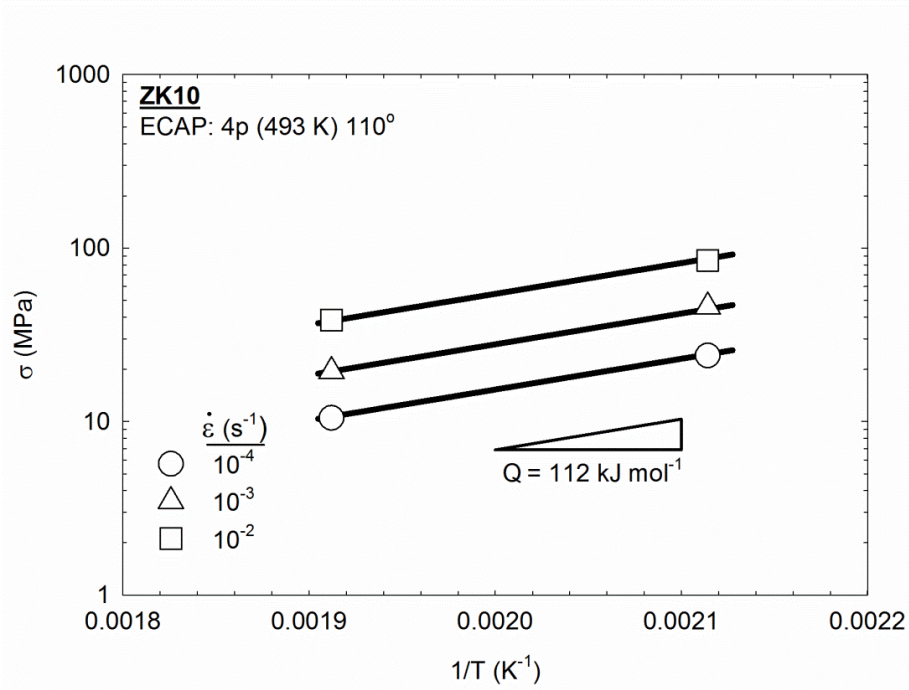

(b)

Figure 5 – (a) Strain rate plotted as a function of stress and (b) stress plotted as a function of the inverse of temperature.

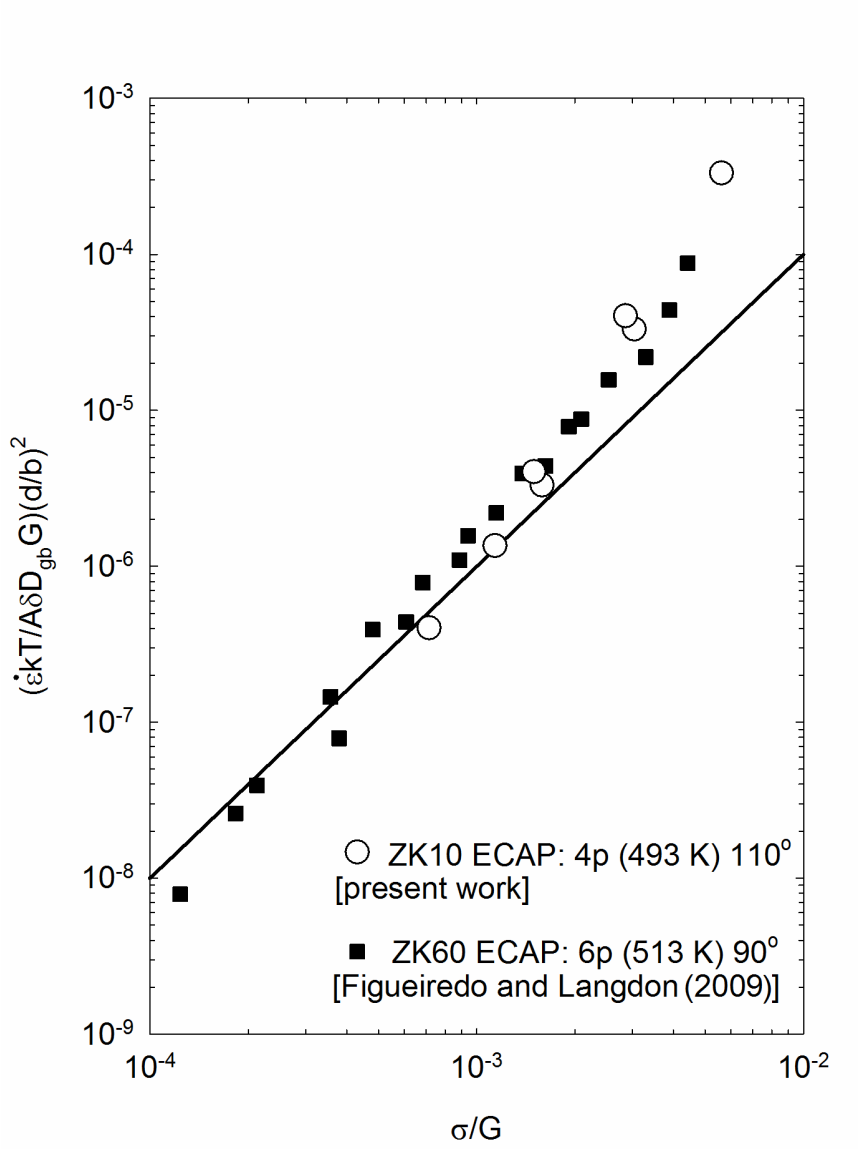

Figure 6 – Strain rate normalized by the effect of temperature and grain size and plotted as a function of the stress normalized by the shear modulus: the theoretical prediction for grain boundary sliding in superplasticity [46] and data from an earlier report [50] are shown for comparison.